Available online at www.sciencedirect.com
SCIENCE DIRECT®
Surface Science 538 (2003) 147–159
SURFACE SCIENCE
www.elsevier.com/locate/susc

Adsorption and reaction of acetaldehyde on Pt(1 1 1) and Sn/Pt(1 1 1) surface alloys

Haibo Zhao, Jooho Kim, Bruce E. Koel *

Department of Chemistry, University of Southern California, Los Angeles, CA 90089-0482, USA

Received 21 March 2003; accepted for publication 22 April 2003

Abstract

Adsorption and reaction of acetaldehyde (CH_3CHO) on Pt(1 1 1) and two ordered Pt–Sn alloys has been studied primarily by using temperature-programmed desorption (TPD) mass spectrometry and high-resolution electron-energy loss spectroscopy (HREELS). The two alloys investigated were the (2×2) and ($\sqrt{3} \times \sqrt{3}$)*R*30°Sn/Pt(1 1 1) surface alloys with $\theta_{Sn} = 0.25$ and $\theta_{Sn} = 0.33$, respectively, as-prepared by vapor deposition of Sn on a Pt(1 1 1) single-crystal substrate. The desorption products in TPD experiments following CH_3CHO exposures on the Pt(1 1 1) surface were CH_3CHO, CO, H_2, and CH_4. Auger electron spectroscopy (AES) detected some carbon ($\theta_C \sim 0.1$ ML) left on the surface following TPD experiments. At small coverages, CH_3CHO adsorption on Pt(1 1 1) is completely irreversible and all CH_3CHO decomposes during heating in TPD. At near monolayer coverages, CH_3CHO is partially reversibly adsorbed, with desorption competing effectively with decomposition so that 52% of the adsorbed monolayer of acetaldehyde decomposed during heating in TPD. CH_3CHO bonds molecularly, mainly in a η^1(O) configuration on Pt(1 1 1) at 90 K. On both of the (2×2)Sn/Pt(1 1 1) and ($\sqrt{3} \times \sqrt{3}$)*R*30°Sn/Pt(1 1 1) alloys, no CH_3CHO decomposition took place during TPD and the adsorption–desorption behavior was entirely reversible. HREELS revealed that only η^1(O)-CH_3CHO was present on the two Sn/Pt(1 1 1) alloys. CH_3CHO is adsorbed more weakly and the chemical reactivity of CH_3CHO on these Sn/Pt alloys is decreased from that on the Pt(1 1 1) surface. Thus, the presence of Sn in the surface layer of these Pt–Sn alloys does not thermally activate acetaldehyde for reaction in UHV due to the thermodynamic driving force provided by the Sn–O interaction. We attribute this to be primarily because of kinetic barriers that arise from Pt–Sn bonding interactions in the alloy and acknowledge the important implications of this observation for the synthesis of organic molecules by selective oxidation over PtSn catalysts.

Keywords: Chemisorption; Alloys; Electron energy loss spectroscopy (EELS); Platinum; Metallic surfaces; Thermal desorption

1. Introduction

Reactions of aldehydes on transition metal surfaces are of interest for a variety of applications. In general, formation of acyl ligands (RC(O)–) via CO insertion into hydrocarbon-surface bonds on metals and the subsequent acyl hydrogenation to produce aldehydes are critical steps in oxygenate

* Corresponding author. Tel.: +1-213-740-4126; fax: +1-213-740-3972.
E-mail address: koel@cheml.usc.edu (B.E. Koel).

0039-6028/03/$ - see front matter © 2003 Elsevier B.V. All rights reserved.
doi:10.1016/S0039-6028(03)00602-2

synthesis [1–3]. Also, there has been a strong interest in developing new catalysts for the selective hydrogenation of α, β-unsaturated aldehydes, e.g., crotonaldehyde [4,5]. Pt and bimetallic Pt catalysts have been investigated in this regard, and a focus has been on increasing the C=O function binding energy at the surface [5,6]. In another application, acetaldehyde is a pollutant in the exhaust from vehicles operated on pure ethanol fuel [7,8], and 0.1 wt.% Pt supported on alumina has been shown to be an efficient catalyst to oxidize acetaldehyde to CO_2 and H_2O [8]. Thus, improved fundamental understanding of aldehyde adsorption and reaction on Pt and Pt alloy surfaces should be helpful for developing catalysts for higher oxygenate synthesis from CO and H_2, selective hydrogenation, and acetaldehyde oxidation for pollution control.

Aldehydes adsorb on metal surfaces by bonding either through the oxygen lone pair electrons in a η^1(O) configuration or in a η^2(C,O) configuration where both the carbonyl carbon and oxygen atoms interact with surface metal atoms. In general, electron donation from the oxygen lone pair orbitals produces a relatively weak surface-adsorbate bond and, as a result, these molecules desorb molecularly at low temperatures. When CH_3CHO binds to a metal surface in a η^2(C,O) state, overlap between the metal d orbitals and the carbonyl π^* orbital is sufficient to allow substantial electron donation from the metal to the carbonyl π^* orbital. This type of back-bonding in the η^2 configuration results in stronger metal–aldehyde bonding and weaker C=O bonding which ultimately leads to a competition between desorption and decomposition reactions. Both η^1(O) and η^2(C,O) configurations have been observed on Pd(1 1 1) [9], Pd(1 1 0) [10], Ru(0 0 1) [11] and Ni(1 0 0) [12] surfaces. Only η^2(C,O)-bonded species were observed on Rh-(1 1 1) [13] and Pt(S)-[6(1 1 1)×(1 0 0)] [14] surfaces.

Surprisingly, there have been no previous surface science studies reported for acetaldehyde adsorption on any Pt surface other than on the stepped surface, Pt(S)-[6(1 1 1)×(1 0 0)] [14]. These results however provide a useful reference for this work. Acetaldehyde adsorbed on Pt(S)-[6(1 1 1)×(1 0 0)] mainly in a η^2(C,O)–π-bonding configuration, with some acetaldehyde molecules adsorbed in a η^2(C,O)–di-σ bonding configuration. Two reaction pathways were proposed by these authors and some acetaldehyde decomposed to form CO, H_2, CH_4, and adsorbed carbon in TPD experiments. As another reference for this work, acetone was shown to weakly and reversibly adsorb and desorb molecularly from Pt(1 1 1) [15].

Alloying Pt with Sn to form the (2×2)Sn/Pt(1 1 1) and $(\sqrt{3}\times\sqrt{3})R30°$Sn/Pt(1 1 1) surface alloys generally decreases the adsorption energy of hydrocarbons and strongly inhibits dehydrogenation reactions, e.g., ethylene [16], cyclohexane [17], and benzene are completely, reversibly adsorbed on these two alloys. Also, these two Pt–Sn surface alloys were found to chemisorb both methanol and ethanol slightly more weakly than on the Pt(1 1 1) surface [18]. It is an open and interesting question whether or not the presence of Sn in the surface layer of Pt–Sn alloys will activate the chemistry of oxygenates such as acetaldehyde to increase the reactivity over that observed on the Pt(1 1 1) surface.

We report here on investigations of the interaction of acetaldehyde with Pt(1 1 1), (2×2)-Sn/Pt(1 1 1) and $(\sqrt{3}\times\sqrt{3})R30°$Sn/Pt(1 1 1) surfaces. Our objectives were to probe adsorption and reaction of acetaldehyde and evaluate whether the presence of Sn in the surface layer of the Pt–Sn surface alloys leads to an increase in adsorption energy or thermally activates these molecules for reaction due to the thermodynamic driving force provided by the Sn–O interaction.

2. Experimental methods

The experiments were conducted in a three-level, ultrahigh-vacuum chamber with a base pressure of 2×10^{-10} Torr. The top level was equipped with a double-pass cylindrical mirror analyzer (CMA) which was used for Auger electron spectroscopy (AES), and X-ray and ultraviolet photoelectron spectroscopy (XPS) and (UPS). The middle level was equipped with LEED optics and a quadrupole mass spectrometer (QMS) for temperature-programmed desorption (TPD) studies. The bottom level contained a LK2000 spectrometer for high-resolution electron energy loss spectroscopy (HREELS). The Pt(1 1 1) crystal was mounted on

two vertical Ta rods which extended into liquid-nitrogen-cooled copper blocks at the bottom of a differentially pumped *XYZ*-manipulator. A chromel–alumel thermocouple was spot-welded directly to the edge of the crystal. The sample could be cooled to 90 K or resistively heated to 1200 K. The Pt(1 1 1) sample was cleaned by repeated cycles of Ar^+-ion bombardment, annealing in vacuum at 1200 K for 1 min and heating in 5×10^{-8} Torr O_2 at 800 K. The cleanliness and long-range order of surfaces were checked by AES and LEED.

Acetaldehyde (Alfa Aesar, 98.5%) was placed in a glass reservoir attached to a stainless-steel dosing line and used as supplied after degassing by multiple freeze–pump–thaw cycles. The acetaldehyde was exposed on the Pt crystal by a microcapillary array doser connected to the gas line through a leak valve. All of the acetaldehyde exposures reported here are given simply in terms of the pressure measured by the ion gauge. No attempt was made to correct for the flux enhancement of the doser or ion gage sensitivity. The mass spectrometer in the chamber was used to check the purity of the gases during dosing.

For all TPD experiments, the heating rate was 3.7 K/s. The HREELS spectra were recorded in the specular direction at an angle of 60° from the surface normal and a primary beam energy of 4.5 eV. The overall energy resolution of the spectrometer was about 50 cm^{-1} and the count rate in the elastic peak was about 10^5 cps for clean Pt(1 1 1).

The (2×2)Sn/Pt(1 1 1) and $(\sqrt{3}\times\sqrt{3})R30°$Sn/Pt(1 1 1) surface alloys were prepared by evaporating Sn onto the Pt(1 1 1) crystal surface and subsequently annealing the sample to 1000 K for 10 s. Depending on the initial, deposited Sn coverage, the annealed surface exhibited either a (2×2) or $(\sqrt{3}\times\sqrt{3})R30°$ pattern in LEED [19]. Sn on these surfaces prepared as above is incorporated substitutionally into these surface layer to form an alloy with $\theta_{Sn}=0.25$, corresponding to the (1 1 1) face of Pt_3Sn, and $\theta_{Sn}=0.33$, corresponding to a Pt_2Sn surface. Sn atoms protrude 0.02 nm above the surface-Pt plane for both surfaces [20]. For the (2×2) structure, pure-Pt threefold sites are present, but no adjacent pure Pt threefold sites exist. All pure-Pt threefold sites are eliminated in the $(\sqrt{3}\times\sqrt{3})R30°$ structure. For brevity throughout this paper, we will refer to the p(2×2)-Sn/Pt(1 1 1) and $(\sqrt{3}\times\sqrt{3})R30°$Sn/Pt(1 1 1) surface alloys as the (2×2) and $\sqrt{3}$ alloys respectively.

3. Results

3.1. Acetaldehyde adsorption on Pt(1 1 1)

TPD spectra for acetaldehyde desorption following acetaldehyde exposures on Pt(1 1 1) at 90 K are shown in Figs. 1 and 2. After very small doses (0.01 and 0.02 L), no molecular CH_3CHO desorption was detected during heating in TPD. In the adsorbed layer formed by exposures larger than 0.03 L, there was competition between molecular desorption and decomposition during TPD. After 0.03 L exposure, CH_3CHO desorbed molecularly in a peak at 200 K. This peak grew larger at constant temperature with increasing acetaldehyde exposures and was very narrow with

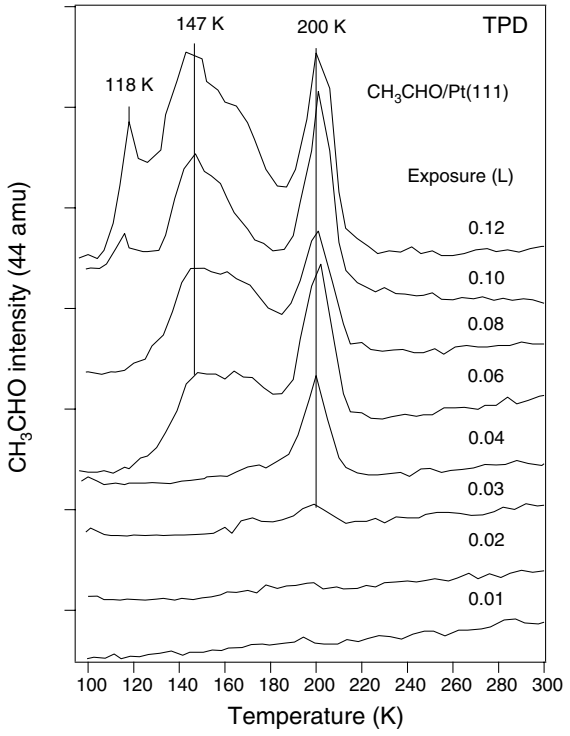

Fig. 1. CH_3CHO TPD spectra after acetaldehyde exposures on Pt(1 1 1) at 90 K.

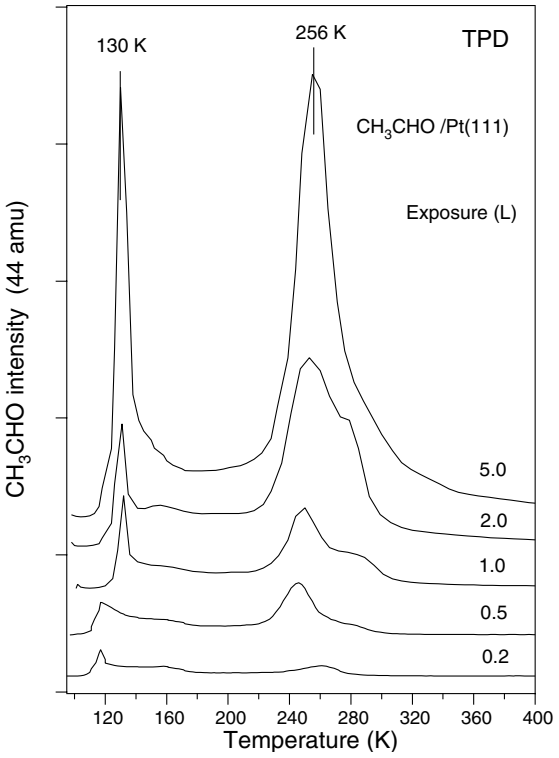

Fig. 2. CH_3CHO TPD spectra after acetaldehyde exposures on Pt(1 1 1) at 90 K.

a 15 K full-width-at-half-maximum (FWHM). A broad desorption feature from 140 to 180 K was observed near saturation coverage in the monolayer, which was reached after a dose of 0.06–0.08 L. Exposures larger than 0.10-L CH_3CHO caused a multilayer peak to appear near 118 K.

After large doses of more than 0.2 L, new TPD peaks appeared near 250 K. Similar results were observed previously on the Ru(0 0 1) surface [11]. We detected the desorption of dimers ($m/e = 88$), trimers ($m/e = 132$) and higher polymers of CH_3CHO in TPD at the same temperature. This indicates that these high temperature peaks arise from depolymerization of $(CH_3CHO)_n$ oligomers in the overlayer. We note that when a very large exposure was given on the surface at 150 K, no CH_3CHO TPD peaks near 250 K were detected. This shows that formation of $(CH_3CHO)_n$ oligomers is dependent on the presence of the acetaldehyde multilayer.

Fig. 3 shows the main desorption products from Pt(1 1 1) after a 0.06-L CH_3CHO dose to produce a coverage of near 1 ML. All masses from 2 to 46 amu were scanned during the TPD experiment. The main products (in addition to acetaldehyde) detected in TPD were 28 amu (CO), 16 amu (CH_4), and 2 amu (H_2). The primary H_2 desorption peak near 360 K arises at least in part from the recombination of hydrogen adatoms on the Pt surface in a desorption rate-limited process. H_2 desorbing in a broad feature from 400 to 700 K is due to reaction rate-limited processes liberating H_2 from decomposition of hydrocarbon fragments on the surface. CO also desorbs in a desorption rate-limited peak at 416 K. The position and shape of the CH_4 desorption peak at 360 K was identical to that of H_2, and occurs at a higher temperature than the CH_4 desorption peak from hydrogenation of adsorbed methyl groups on Pt(1 1 1) which occurs at or below 295 K [21–24]. Thus, CH_4 desorption after CH_3CHO exposures is rate-limited

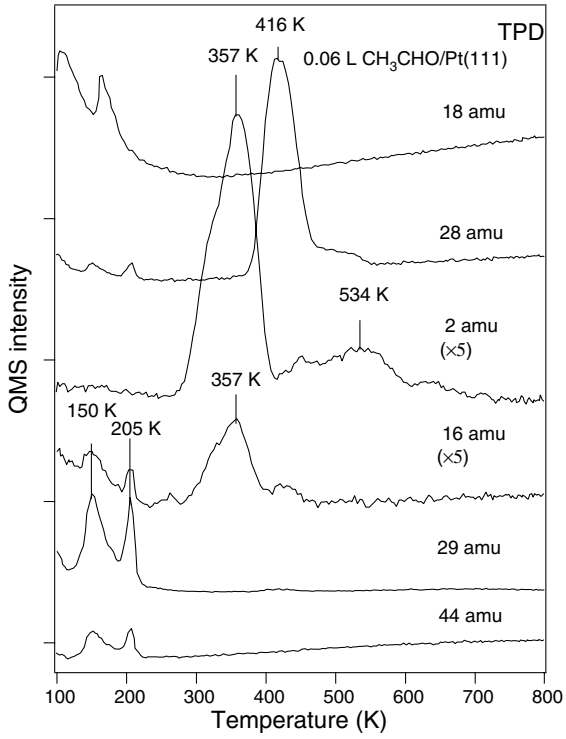

Fig. 3. TPD spectra obtained from signals at 29, 44, 2, 16, 28, and 18 amu after a 0.06-L CH_3CHO exposure on Pt(1 1 1) at 90 K.

by the formation of adsorbed CH_3 species. A H_2O peak desorbs at 162 K, but we believe that this peak comes from water coadsorption from the background gas rather than as a product of CH_3CHO decomposition because we observed the same size of H_2O peak at the same temperature on the Sn/Pt(1 1 1) surface alloys (on which CH_3CHO does not decompose).

Fig. 4 shows the yields for CO, H_2, CH_4 and the CH_3CHO as constructed from TPD peak areas following CH_3CHO adsorption on the Pt(1 1 1) surface at 90 K. The amount of CO, H_2, CH_4 products from decomposition and the amount of desorption of chemisorbed CH_3CHO reached a maximum after 0.07 L exposure. This indicates that a 0.07-L exposure forms 1 ML of CH_3CHO on the Pt(1 1 1) surface. The number of η^1(O)-CH_3CHO molecules (see below for assignment) that occupy the monolayer can be estimated to be 0.36 ML for close-packing of molecules with their van der Waals radii. This value can be checked by consideration of the amount of decomposition products desorbed in TPD. The amount of CO desorbed from Pt(1 1 1) can be calculated by comparing the CO TPD area after CH_3CHO exposures to that from CO exposures on Pt(1 1 1). The saturation coverage of CO on Pt(1 1 1) is 0.68 ML at 150 K [25] and, using TPD, we checked that the amount of CO adsorbed on Pt(1 1 1) at 90 K is the same as that at 150 K. The total CH_3CHO uptake curve in Fig. 4 includes the amount of CH_3CHO decomposed and that desorbed molecularly from the monolayer. Stoichiometry provides that decomposition of one molecule of CH_3CHO will produce one molecule of CO, and so we can use the CO TPD area plus the desorbed CH_3CHO TPD area multiplied by some coefficient to give the total CH_3CHO uptake that is required to keep the sticking coefficient of CH_3CHO constant. Polymerization prevents us from constructing the CH_3CHO uptake curve for multilayer coverages. From a quantitative analysis of the amount of CO desorbed from CH_3CHO decomposition, we estimate that the monolayer CH_3CHO coverage corresponds to 5.3×10^{14} cm^{-2} or 0.35 ML defined with respect to the Pt(1 1 1) surface atom density. This value agrees well with our previous estimate. By assuming a constant value of the sticking coefficient of acetaldehyde on Pt(1 1 1) at 90 K over this coverage range, we calculate that 52% of the adsorbed acetaldehyde decomposes during TPD at monolayer coverage.

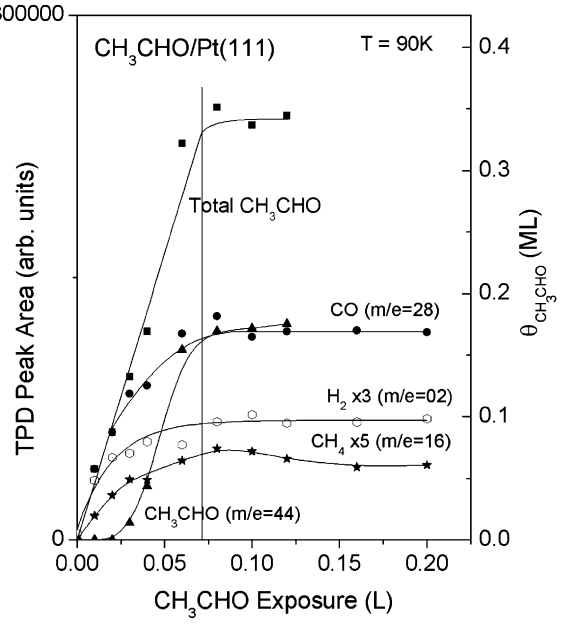

Fig. 4. Uptake curves constructed from the TPD-peak areas following the adsorption of CH_3CHO on Pt(1 1 1) at 90 K.

HREELS spectra obtained after various CH_3CHO exposures on Pt(1 1 1) at 90 K are shown in Fig. 5. Several physisorbed layers of CH_3CHO are formed by a 0.5-L CH_3CHO exposure, and HREELS spectra from the condensed film are similar to IR spectra of crystalline CH_3CHO. Table 1 lists the vibrational frequencies (cm^{-1}) and mode assignments for crystalline acetaldehyde [26], acetaldehyde coordinated in a metal complex, i.e., an acetaldehyde–solvated Ni complex, and at several metal surfaces. Spectra taken after 0.05- and 0.07-L exposures to give monolayer coverages have loss peaks at 2984, 1667, 1430, 1365, 1130, 913, and 550 cm^{-1}. After a 0.05-L exposure, the carbonyl-stretching mode shifted from 1734 to 1667 cm^{-1}. In the acetaldehyde–solvated nickel complex $Ni(CH_3CHO)_6(FeCl_4)_2$, acetaldehyde molecules form weak donor bonds to the Ni atom through the oxygen atom and the carbonyl stretch of CH_3CHO occurs at 1665 cm^{-1} in this complex [27]. This value is close to that of chemisorbed

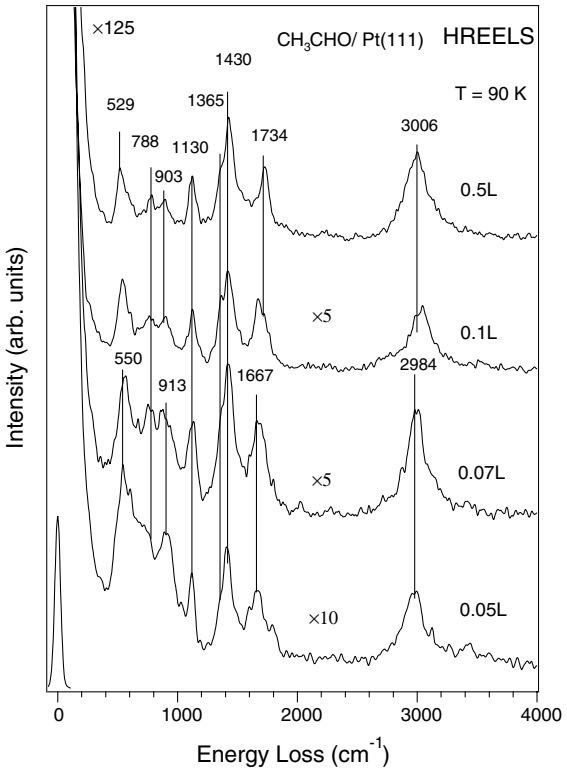

Fig. 5. HREELS spectra after CH_3CHO exposures on Pt(1 1 1) at 90 K.

CH_3CHO on Pt(1 1 1), and therefore we assign a bonding geometry of η^1(O)-CH_3CHO to acetaldehyde adsorbed in the monolayer on Pt(1 1 1) at 90 K. Previous isotope-labeling studies showed that the losses in HREELS at 1380 and 1450 cm^{-1} were from the ν(CO) modes of η^2(C,O)-CH_3CHO on Ru(0 0 1) [11] and Rh(1 1 1) [13], respectively. However, in the absence of such information, interference by the methyl deformation modes of acetaldehyde between 1380 and 1430 cm^{-1} [10] prevents the use of Fig. 5 to identify the ν(CO) modes of η^2(C,O)-CH_3CHO.

In order to interpret the HREELS spectra presented below, we obtained a set of TPD curves after annealing the surface produced by a fixed, 0.2-L CH_3CHO exposure on Pt(1 1 1) at 90 K. The results are shown in Fig. 6 for molecular acetaldehyde desorption (as monitored by the signal at 44 amu). Some physisorbed CH_3CHO remains on the Pt(1 1 1) surface after annealing to 120 K, but this was removed completely after heating to 150 K. Two molecular desorption peaks were observed in TPD after annealing to 150 K, but only one CH_3CHO desorption peak was left after annealing to 200 K. After heating to 300 K, no molecular CH_3CHO desorption was detected in the subsequent TPD experiment.

Table 1
Vibrational frequencies (cm^{-1}) and mode assignments for acetaldehyde (CH_3CHO)

Mode description	IR		HREELS				
	Crystalline [26]	$Ni(CH_3CHO)_6$–$(FeCl_4)_2$ [27]	Pt(1 1 1), 90 K, This work	(2×2) alloy, 90 K, This work	$\sqrt{3}$ alloy, 90 K, This work	Ru(0 0 1), 110 K [11]	Rh(1 1 1), 143 K [13]
$\nu_a(CH_3)$	3003; 2964		2984	3012	3012		
$\nu_s(CH_3)$	2918					2970	2980
ν(CH)	2747					nr	
ν(CO)	1722	1665	1667	1692	1713		1460
$\delta(CH_3)$	1431		1430	1433	1430	1395	1380
$\delta_{as}(CH_3)$	1422						
δ(CH)	1389		1365	1365	1365		
$\delta_s(CH_3)$; ν(CH)	1347						
$\rho(CH_3)$; ν(CC)	1118	1130	1130	1133	1130		
ρ(CH); $\rho(CH_3)$	1102						
ν(CC); $\rho(CH_3)$	882	n.o.	913	908	908	915	950
ρ(CH); $\rho(CH_3)$	770			786	717		
δ(CCO)	552	568	607			605	610
γ(M–C)		282	550	539	531		

nr = not resolved.

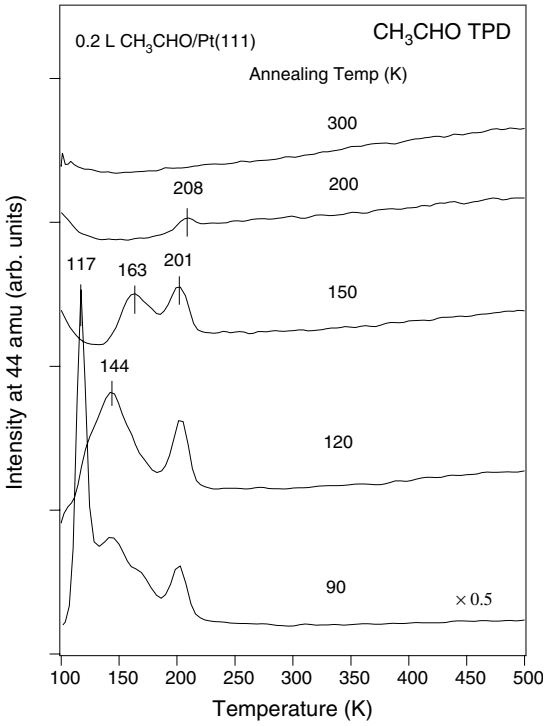

Fig. 6. CH_3CHO TPD spectra after heating following a 0.2-L CH_3CHO exposure on Pt(1 1 1) at 90 K.

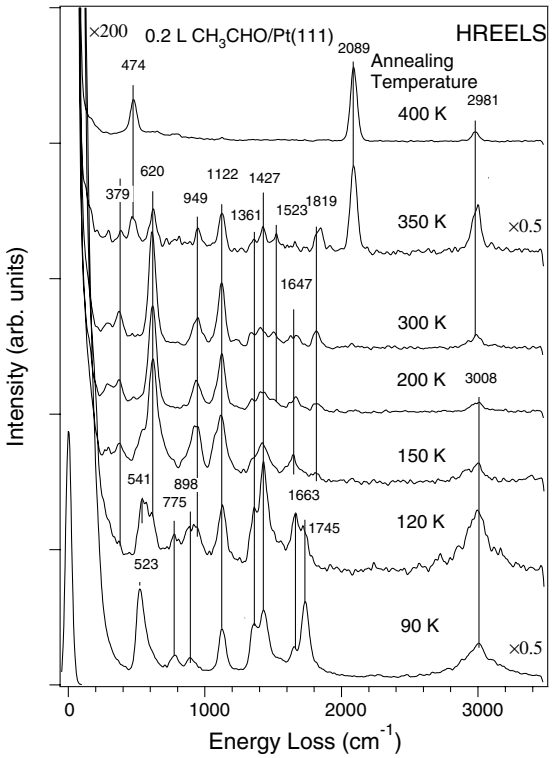

Fig. 7. HREELS spectra after heating following a 0.2-L CH_3CHO exposure on Pt(1 1 1) at 90 K.

Fig. 7 shows HREELS spectra after acetaldehyde exposures and annealing procedures identical to those utilized in producing Fig. 6. Upon increasing the temperature from 90 to 120 K, the peak at 1745 cm^{-1} decreased in intensity and the peak at 523 cm^{-1} shifted to 541 cm^{-1}. This change is associated with desorption of multilayer CH_3CHO. The peak at 1663 cm^{-1} arises from chemisorbed CH_3CHO. The peak at 1663 cm^{-1} increased in intensity and a new peak at 620 cm^{-1} appeared. Annealing to 150 K caused peaks at 541 and 1745 cm^{-1} to nearly disappear, the peak at 1663 cm^{-1} to shift to 1647 cm^{-1}, and the peak at 620 cm^{-1} to increase strongly in intensity. Only small additional changes occurred in the HREELS spectra after heating to 200 or 300 K, which included the appearance of small peak at 1523 cm^{-1}. However, after annealing to 350 K, the ν(CO) and ν(Pt–CO) modes of atop-bonded CO were observed at 474 and 2089 cm^{-1} and a small amount of bridge-bonded CO was also indicated by a loss peak at 1819 cm^{-1}. Heating to 350 K also caused the peaks at 620 and 1647 cm^{-1} to decrease in size and the ν(CH) stretching peak at 2981 cm^{-1} to increase in intensity. After heating to 400 K, only small loss peaks remain due to residual adsorbed hydrocarbon species, and HREELS primarily detected remaining atop-bonded CO.

3.2. Acetaldehyde adsorption on Sn/Pt(1 1 1) surface alloys

A series of TPD spectra for acetaldehyde desorption from the (2×2) and $\sqrt{3}$ surface alloys are shown in Figs. 8 and 9, respectively, after acetaldehyde exposures were given on each surface at 90 K. In each case, a separation occurred between a high-temperature desorption peak from a chemisorbed state and a low-temperature desorption peak from physisorbed states. After large exposures, high-temperature desorption peaks at 243

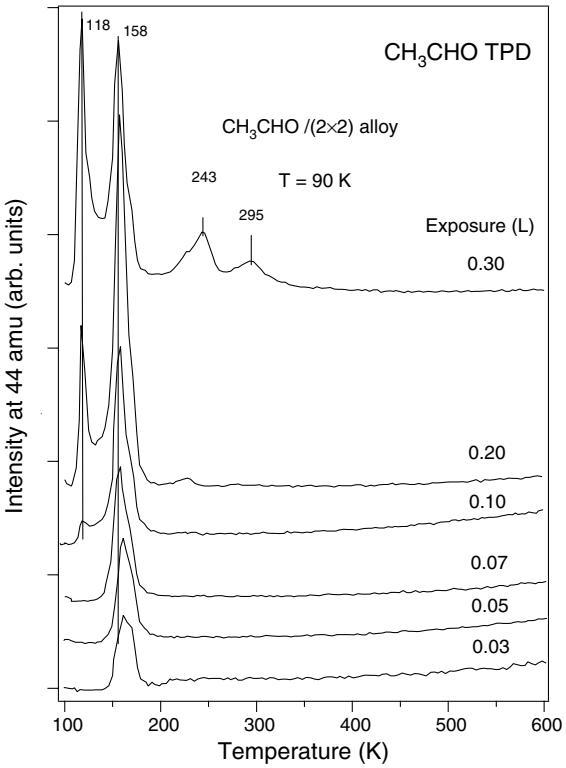

Fig. 8. CH_3CHO TPD spectra after acetaldehyde exposures on the (2×2)Sn/Pt(1 1 1) surface alloy at 90 K.

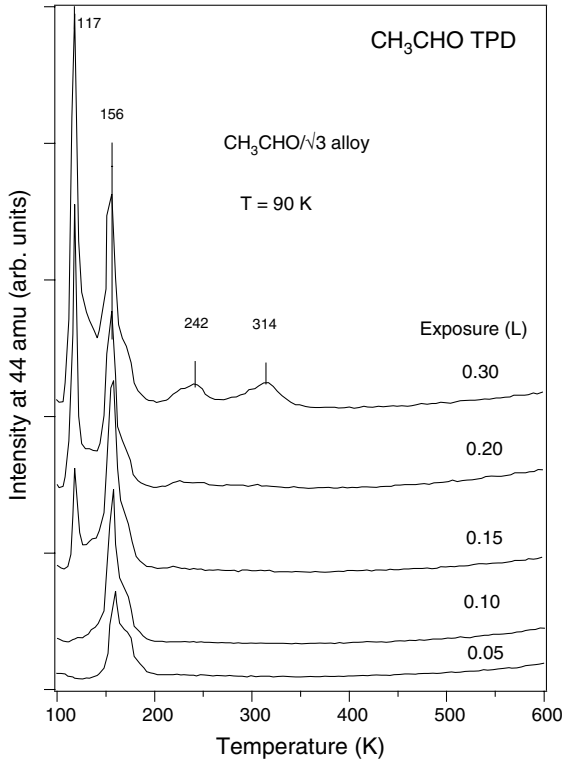

Fig. 9. CH_3CHO TPD spectra after acetaldehyde exposures on the $(\sqrt{3} \times \sqrt{3})R30°$Sn/Pt(1 1 1) surface alloy at 90 K.

and 295 K from depolymerization of a $(CH_3CHO)_n$ layer were observed. Physisorbed molecules that eventually form the condensed phase, multilayer desorption peak after large exposures desorb at 118 K on both of these two surface alloys, just as on Pt(1 1 1). The desorption peak from chemisorbed CH_3CHO species was similar on both surface alloys. On the (2×2) alloy, the peak appeared at 161 K and shifted to 158 K at monolayer coverage. On the $\sqrt{3}$ alloy, the peak appeared at 160 K and shifted to 158 K at monolayer coverage. The narrow peaks and small shifts in the TPD peak maximum with increasing acetaldehyde coverage on both of these surfaces indicates first-order desorption kinetics and simple reversible, molecular acetaldehyde adsorption on both alloys. While signals for CO, H_2 and CH_4 evolution from possible acetaldehyde decomposition were monitored during TPD from both alloys, no appreciable signals were detected. Thus, no decomposition occurs under these conditions on the two alloys. Consistent with these TPD results, no carbon or oxygen was detected by AES following TPD experiments.

A direct comparison of CH_3CHO desorption in TPD from the acetaldehyde monolayer on all three surfaces is shown in Fig. 10. These spectra illustrate the influence of alloyed Sn in changing the nature of acetaldehyde adsorption. There is no peak at 200 K on the two Pt–Sn alloys. This peak on Pt(1 1 1) is caused by recombination of coadsorbed acetyl groups and H adatoms, as we will establish below. Assuming first-order kinetics with a preexponential factor of 10^{13} s^{-1}, the Redhead method [28] can be used to estimate a desorption activation energy E_d for acetaldehyde adsorbed in the monolayer on the two alloy surfaces of $E_d = 9.5$ kcal/mol. However, E_d of acetaldehyde adsorbed at 148 K in the monolayer on the Pt(1 1 1) is estimated as 8.88 kcal/mol, which is

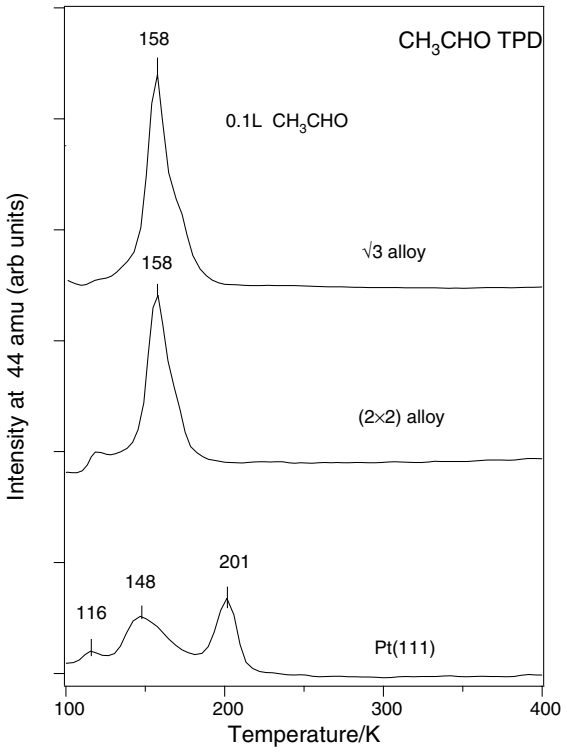

Fig. 10. Comparison of CH_3CHO desorption from chemisorbed monolayers on Pt(1 1 1) and Pt–Sn alloy surfaces.

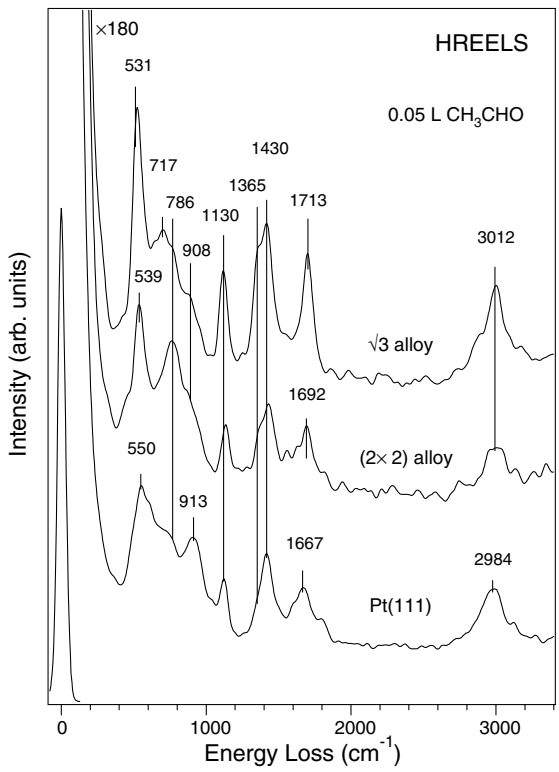

Fig. 11. Comparison of vibrational spectra from HREELS after 0.05-L CH_3CHO exposures to give near monolayer coverage on Pt(1 1 1) and Pt–Sn alloy surfaces.

affected by the decomposition of acetaldehye at this temperature. The recombinative peak at 201 K places a lower limit on E_d for the desorption of η^1(O)-CH_3CHO on Pt(1 1 1) of 13 kcal/mol.

It appears that the desorption temperature of η^1(O)-CH_3CHO on Pt(1 1 1) at 148 K is close to the desorption temperature of η^1(O)-CH_3CHO on the (2×2) and $\sqrt{3}$ alloy surfaces. The HREELS spectra obtained from Pt(1 1 1) and the (2×2) and $\sqrt{3}$ alloys at 90 K at low coverages of acetaldehyde, as shown in Fig. 11, are similar. The ν(CO) stretching vibration is at 1667, 1692 and 1713 cm^{-1} on Pt(1 1 1) and the (2×2) and $\sqrt{3}$ alloys, respectively. These frequencies are typical for η^1(O)-CH_3CHO species. Increasing the Sn concentration in the surface alloy shifts the CO stretching vibration closer to the frequency of condensed phase, crystalline CH_3CHO. There are also subtle changes in the intensities of the ν(CO) and $\delta(CH_3)$ modes due to alloying Sn with Pt. These are likely caused by changes in the orientation of the acetaldehyde molecule at the surface, but some changes are expected particularly in the ν(CO) mode because of the weaker interaction at the alloy surface.

4. Discussion

Acetaldehyde chemisorbs on Pt(1 1 1) at 90 K mainly in a bonding geometry of η^1(O)-CH_3CHO. This assignment was made by using HREELS spectra from chemisorbed CH_3CHO on Pt(1 1 1) and is based on the close agreement between the carbonyl stretching frequencies in this species and that in a $Ni(CH_3CHO)_6(FeCl_4)_2$ complex in which acetaldehyde molecules form weak donor bonds to the Ni atom through the oxygen atom. Previous semiempirical extended Hückel calculations [29] had predicted that the η^2(C,O) configuration was

the preferred adsorption geometry of formaldehyde and acetaldehyde on Pt(1 1 1), Pt(1 1 0), and stepped Pt(1 1 1) surfaces.

The bonding of acetaldehyde on Pt(1 1 1) appears to be weaker than on the other transition metal surfaces studied thus far, since an η^2(O)-CH_3CHO species, which is more strongly rehybridized from the gas phase molecule, has been proposed to form on Ru(0 0 0 1) [11], Rh(1 1 1) [13], and Pd(1 1 1) [9] and (1 1 0) [10] surfaces. In the latter three cases, it was suggested that an η^1(O)-CH_3CHO species could also be formed at less than 150 K. However, even though we can clearly rule out η^2(C,O)-CH_3CHO on Pt(1 1 1) as the dominant species, interferences in the spectra make it impossible for us without isotopic labeling to identify the ν(CO) modes of a small amount of η^2(C,O)-CH_3CHO on Pt(1 1 1) that might be present in the present study.

Heating η^1(O)-CH_3CHO species on Pt(1 1 1) to 150 K causes partial dehydrogenation at the α-C–H bond to form chemisorbed acetyl (η^1(C)-CH_3CO) groups, and no molecular acetaldehyde species remains coadsorbed on the surface. The acetyl identification was made by comparing our HREELS spectra to the IR spectrum of a trans-$[PtBr(COCH_3)(PEt_3)_2]CCl_4$ complex which shows a ν(CO)-acetyl band at 1630 cm^{-1} [30], as listed in Table 2. This is close to a peak at 1647 cm^{-1} that we assigned to the ν(CO) mode of surface-bound acetyl groups on Pt(1 1 1). The bonding of acetyl groups on Pt(1 1 1), and also on Pt(S)-[6(1 1 1)×(1 0 0)] where the ν(CO)-acetyl band is at 1650 cm^{-1}, more closely resembles that in the complex than does acetyl species bonded on Pd(1 1 1) and (1 1 0) surfaces where the ν(CO)-acetyl band was assigned to peaks at 1565 and 1610 cm^{-1}, respectively.

Heating an acetaldehyde adlayer on Pt(1 1 1) to 350 K causes decarbonylation. This is evident by the appearance of ν(CO) modes at 2089 and 1819 cm^{-1} due to adsorbed CO. Over the temperature range of 150–300 K, almost no changes were observed in the HREELS spectra. That means surface-bound acetyl intermediates are quite stable. Chemisorbed acetyl species decarbonylate at 300–350 K to release CO and a C_1 species adsorbed on the surface. TPD experiments after a 0.06-L acetaldehyde dose on Pt(1 1 1) showed methane (CH_4) desorption at temperatures higher than those required for methyl group disproportionation/hydrogenation [24], and so CH_4 evolution is rate-limited by acetyl decarbonylation. The presence of surface hydrogen from acetyl formation means that most methyl groups on the surface are hydrogenated to form methane during TPD, but a small fraction does dehydrogenate further to deposit carbon on the surface.

It is of interest to compare the reactivity of the Pt(1 1 1) surface with that of a stepped Pt surface to assess the role of steps and defects. CH_3CHO adsorption on a Pt(S)-[6(1 1 1)×(1 0 0)] surface was investigated previously [14]. On both the (1 1 1) and stepped Pt surfaces, acetaldehyde adsorbs molecularly at low temperatures and dehydrogenates to desorb CO, H_2 and CH_4 at high temperatures. However, Madix et al. [14] reported that acetaldehyde adsorbs only in a η^2(C,O)-CH_3CHO config-

Table 2
Vibrational frequencies (cm^{-1}) and mode assignments for acetyl (CH_3CO) ligands

Mode description	IR	HREELS			
	trans-$[PtBr(CO\text{-}CH_3)(PEt_3)_2]$ in CCl_4 [30]	Pd(1 1 0), 150 K [10]	Pd(1 1 1), 150 K [9]	Pt(S)-[6(1 1 1)×(1 0 0)], 154 K [14]	Pt(1 1 1), 150 K, This work
$\nu_a(CH_3)$		2985	2990		2984
ν(CO)	1630	1610	1565	1650	1647
$\delta_{as}(CH_3)$		1406	1390		1427
$\delta_s(CH_3)$		1334			1361
ν(CC)		1076	1080	1120	1122
$\rho(CH_3)$	909	918	900	900–925	949
δ(CCO)	584	595	600	610	620
ν(M–C)	537	330; 445	330		379

uration and ruled out an η^1(O)-CH_3CHO configuration by using HREELS on the stepped Pt surface. They also assigned the main acetaldehyde desorption peak at 237 K to be mainly from π–η^2(C,O)-CH_3CHO and a minor desorption peak at 258 K to arise from desorption of di-σ–η^2(C,O)-CH_3CHO. They did not identify any intermediate from partial dehydrogenation to be formed as a stable species on the surface. Because of the limitations of this work, we cannot make too many conclusions. However, it appears that step sites are indeed more reactive than Pt(1 1 1) terrace sites and this would account for the formation of strongly bound di-σ–η^2(C,O)-CH_3CHO species and a higher reactivity for chemisorbed acetyl species.

On Pt(1 1 1), we observed CH_3CHO desorption in TPD in a peak at 200 K. We assign this peak to arise from the recombination of coadsorbed H adatoms and acetyl groups rather than desorption of strongly bound di-σ–η^2(C,O)-CH_3CHO species. In addition to our HREELS spectra, this assignment is consistent with TPD results after CH_3CHO adsorption on the two Pt–Sn alloys. On these alloys, there is no acetaldehyde decomposition and no CH_3CHO TPD peak near 200 K.

Desorption peaks of acetaldeyde molecules from Pt(1 1 1) at temperatures higher than 210 K in TPD experiments are from depolymerization of $(CH_3CHO)_n$ species, as has been reported on Ru(0 0 1) [11], S-covered Ni(1 0 0) [12] and some oxide surfaces [31]. Henderson et al. [11] reported that CH_3CHO polymerizes in two dimensions upon adsorption on Ru(0 0 1) even at low exposures. They excluded the possibility of η^2(C,O)-CH_3CHO bound on Ru(0 0 1) at temperatures lower than 250 K, but allow for the formation of this species by decomposition of polymers at higher temperature. They also proposed that η^1(O)-CH_3CHO species exist at larger exposures, but incorporate into the surface polymer below 150 K.

In studies on a related molecule, acetone (CH_3COCH_3), Ibach et al. [15] observed both η^1(O)-CH_3COCH_3 and η^2(C,O)-CH_3COCH_3 configurations in the monolayer of acetone on Pt(1 1 1). In TPD experiments, they reported that η^1(O)-CH_3COCH_3 desorbed at 184 K and η^2(C,O)-CH_3COCH_3 desorbed around 200 K. No decomposition of acetone was reported. Thus, acetaldehyde is a more reactive molecule than acetone on Pt(1 1 1). The molecular structure of acetaldehyde differs from acetone in that the methyl group bonded to the central carbon atom in acetone is replaced by an H atom in acetaldehyde. Even though average C–C and C–H bond energies are 348 and 413 kJ/mol, respectively, C–H bond cleavage often has lower barriers than C–C bond cleavage on Pt(1 1 1) [32]. Thus, α-H elimination would be expected to be the first step in decomposition of CH_3CHO on Pt(1 1 1). Indeed, we conclude that α-H elimination forms η^1(C)-acetyl species on Pt(1 1 1) at 150 K. Because acetone should have a C–C bond cleavage barrier that exceeds that of α-H elimination from acetaldehyde on Pt(1 1 1), it is reasonable that acetone would not decompose prior to desorption below 200 K. As a final point, we also mention that acetaldehyde is more reactive than ethanol (CH_3CH_2OH) on Pt(1 1 1) [18]. Ethanol molecules also have α-H's, but do not decompose under UHV conditions on Pt(1 1 1) because of the lack of the acyl (C=O) functional group.

A motivating factor for performing these experiments was to determine if the presence of Sn in Pt–Sn alloys would "activate", i.e. make more reactive, those organic molecules that contained oxygen due to the strong oxophilic nature of Sn. Even though the strong Sn–O bond provides a thermodynamic driving force for decomposition of acetaldehyde, Pt–Sn bonding leads to a energetic barrier that inhibits decomposition over that on clean Pt(1 1 1). Decomposition was completely eliminated on both of the two Sn/Pt(1 1 1) surface alloys and adsorption of acetaldehyde was found to be entirely reversible. Only one chemisorbed CH_3CHO state was found which desorbed in a peak at 158 K in TPD from both surfaces. At low coverages, a strong ν(CO) peak at 1692 cm^{-1} in HREELS can be assigned to a η^1(O)-CH_3CHO species on the (2×2) alloy. With the increase in Sn concentration at the $\sqrt{3}$ alloy surfaces, the ν(CO) peak shifts to 1713 cm^{-1}. These energies are larger than that for the CO stretching mode of CH_3CHO adsorbed on Pt(1 1 1), consistent with a weaker interaction between CH_3CHO and the surface with increasing Sn concentration.

Electronic structure calculations by Pick [33] have shown that bonding interactions between Pt and Sn in Pt–Sn alloy change the local electronic structure at Pt and Sn sites. Hybridization between Pt-d and Sn-p electrons leads to a lowering of the LDOS at the Fermi level and a downward shift of the Pt local d-band. Depopulation of the Pt 5d band evidently leads to the formation of a significant activation energy barrier for bond dissociation reactions of adsorbed molecules, including reactions of oxygen-containing organic molecules. This also weakens the bonding interaction of molecular adsorbates on the alloys. The role of so-called "ensemble effects" that depend on the number of contiguous reactive sites (Pt atoms) at the surface on the (2×2) and $\sqrt{3}$ alloys is difficult to assess, but this is not like to be the primary limitation of CH_3CHO decomposition on the alloys. This assertion stems from our observation that cyclohexadiene (c-C_6H_8) dehydrogenates facilely on both surface alloys [34] and thus electronic effects appear to play a more decisive role in the altered chemical reactivity for acetaldehyde adsorbed on these alloys.

These results on acetaldehyde along with other studies of methanol, ethanol, and water [18], ethylene oxide [35], nitromethane and methyl nitrite [36], are part of a consistent picture that Pt–Sn alloys have smaller chemisorption energies and increased reaction barriers for oxygen-containing molecules compared to Pt surfaces.

5. Summary

At small coverages (below 0.1 ML), acetaldehyde decomposes on Pt(1 1 1) to yield gas phase CO, H_2, CH_4, and deposit some surface carbon during TPD. Molecular desorption also takes place from the adsorbed monolayer at higher CH_3CHO coverages. The chemisorbed layer is populated mostly by η^1(O)-CH_3CHO species on the Pt(1 1 1) surface at 90 K. Adsorbed CH_3CHO thermally decomposes to form surface-bound acetyl groups at 150 K, and some acetyl species are subsequently rehydrogenated and desorb as acetaldehyde at 200 K. Any remaining acetyl groups begin to thermally decompose at 350 K.

Alloying Sn weakens the interaction of acetaldehyde at the surface. Acetaldehyde adsorption on the (2×2) and $(\sqrt{3}\times\sqrt{3})R30°$Sn/Pt(1 1 1) surface alloy is completely reversible, and no decomposition of acetaldehyde occurred during TPD. Only η^1(O)-CH_3CHO species were observed on the two alloys. Even though CH_3CHO desorbed at the same temperature in TPD on the two surface alloys, HREELS spectra show a stronger perturbation of the CH_3CHO molecular chemisorbed on the (2×2) alloy than on the other alloy. We attribute the decrease in the chemical reactivity of these Pt–Sn alloys compared to that of the Pt(1 1 1) surface to be primarily due to electronic effects that arise from Pt–Sn bonding interactions in the alloy.

Acknowledgements

This work was supported by the Department of Energy, Office of Basic Energy Sciences, Chemical Sciences Division.

References

[1] A.T. Bell, Catal. Rev.—Sci. Eng. 23 (1981) 203.
[2] P. Biloen, W.M.H. Sachtler, Adv. Catal. 30 (1981) 165.
[3] V. Ponec, Catalysis (Lond.) 5 (1981) 48.
[4] P.N. Rylander, N. Himelstein, M. Kilroy, Engelhard Ind. Tech. Bull. 4 (1963) 49.
[5] C.G. Raab, J.A. Lercher, J. Mol. Catal. 75 (1992) 71.
[6] Z. Poltarzewski, S. Galvagno, R. Pietropaolo, P. Staiti, J. Catal. 102 (1986) 190.
[7] P. Gunby, J. Am. Med. Assoc. 243 (1980) 1967.
[8] R.S. Goodrich, Chem. Eng. Prog. 78 (1982) 29.
[9] J.L. Davis, M.A. Barteau, J. Am. Chem. Soc. 111 (1989) 1782.
[10] R. Shekhar, M.A. Barteau, R.V. Plank, J.M. Vohs, J. Phys. Chem. B 101 (1997) 7939.
[11] M.A. Henderson, Y. Zhou, J.M. White, J. Am. Chem. Soc. 111 (1989) 1185.
[12] R.J. Madix, T. Yamada, S.W. Johnson, Appl. Surf. Sci. 19 (1984) 43.
[13] C.J. Houtman, M.A. Barteau, J. Catal. 130 (1991) 528.
[14] R.W. McCabe, C.L. DiMaggio, R.J. Madix, J. Phys. Chem. 89 (1985) 854.
[15] M.A. Vannice, W. Erley, H. Ibach, Surf. Sci. 254 (1991) 1.
[16] M.T. Paffett, Surf. Sci. 223 (1989) 449.
[17] C. Xu, Y.L. Tsai, B.E. Koel, J. Phys. Chem. 98 (1994) 585.
[18] C. Panja, N.A. Saliba, B.E. Koel, Surf. Sci. 395 (1998) 248.
[19] M.T. Paffett, R.G. Windham, Surf. Sci. 208 (1989) 34.

[20] S.H. Overbury, D.R. Mullins, M.T. Paffett, B.E. Koel, Surf. Sci. 254 (1991) 45.
[21] M.A. Henderson, G.E. Mitchell, J.M. White, Surf. Sci. 184 (1987) L325.
[22] F. Zaera, H. Hoffmann, P.R. Griffiths, J. Electron. Spec. Relatd. Phenom. 54/55 (1990) 705.
[23] F. Zaera, H. Hoffmann, J. Phys. Chem. 95 (1991) 6297.
[24] C. Panja, N.A. Saliba, E.C. Samano, B.E. Koel, in press.
[25] M.T. Paffett, S.C. Gebhard, R.G. Windham, B.E. Koel, J. Phys. Chem. 94 (1990) 6831.
[26] H. Hollenstein, H.H. Günthard, Spectrochim. Acta A 27 (1971) 2027.
[27] W.L. Driessen, W.L. Groeneveld, Recl. Trav. Chim. Pays-Bas 90 (1971) 87.
[28] P.A. Redhead, Vacuum 12 (1962) 203.
[29] J.M. Pėrez, F.J. Cases, J.L. Vázquez, A. Aldaz, Surf. Sci. 235 (1990) 307.
[30] D.M. Adams, G.J. Booth, Chem. Soc. (1962) 1112.
[31] H. Idriss, C. Diagne, J.P. Hindermann, A. Kiennemann, M.A. Barteau, J. Catal. 155 (1995) 219.
[32] C.T. Campbell, Y.-K. Sun, W.H. Weinberg, Chem. Phys. Lett. 179 (1991) 53.
[33] S. Pick, Surf. Sci. 436 (1999) 220.
[34] J.W. Peck, B.E. Koel, J. Am. Chem. Soc. 118 (1996) 2708.
[35] J. Kim, H. Zhao, B.E. Koel, in press.
[36] J.W. Peck, D.I. Mahon, D.E. Beck, B.E. Koel, Surf. Sci. 410 (1998) 170.